

## RESEARCH ARTICLE

View Article Online  
View Journal

Cite this: DOI: 10.1039/d2qo00851c

# Coupling partner-dependent unsymmetrical C–H functionalization of *N*-phenoxyacetamides leading to sophisticated spirocyclic scaffolds†

Xia Song,<sup>a</sup> Kelin Wang,<sup>a</sup> Lian Xue,<sup>a</sup> Haibo Yu,<sup>b</sup> Xinying Zhang,<sup>b</sup> Richmond Lee<sup>b</sup> and Xuesen Fan<sup>a</sup>

A coupling partner-dependent unsymmetrical C–H bond functionalization of *N*-phenoxyacetamides leading to the formation of sophisticated spirocyclic scaffolds is presented herein. To be specific, spiro-pyrazolonyl indazoles were formed from *N*-phenoxyacetamides and diazopyrazolones through sequential C–H bond cleavage and carbene insertion into two different phenyl moieties. On the other hand, bispiro-oxindoyl dihydrobenzofurans were formed from *N*-phenoxyacetamides and diazooxindoles through C–H bond cleavage and cascade carbene insertion into phenyl and oxindoyl moieties, respectively. These transformations not only provided effective strategies for the synthesis of the otherwise difficult-to-obtain spiroheterocyclic skeletons from simple and readily available substrates in a straightforward and atom-economic manner, but also disclosed some unprecedented reaction modes of *N*-phenoxyacetamides with cyclic diazo compounds. Structural elaborations of the products obtained herein furnished some valuable heptacyclic architectures. Mechanistic experiments and DFT calculations were also carried out to unveil the reaction mechanisms, especially the origin of the excellent chemo-selectivity and diastereoselectivity demonstrated in the formation of bispirooxindoyl dihydrobenzofuran products.

Received 25th May 2022,  
Accepted 11th July 2022

DOI: 10.1039/d2qo00851c

rsc.li/frontiers-organic

## Introduction

Tremendous advances have been made in the development of more practical and efficient synthetic methods towards functional organic molecules, but the pursuit of step-economical methods enabling precise assembly of complex molecular scaffolds is still highly attractive, and the goal of this work is to develop an effective strategy for the design of catalytic cascade reactions enabling the formation of multiple bonds in a one-pot reaction.<sup>1</sup>

Transition metal (TM)-catalyzed and directing group (DG)-assisted functionalization of ubiquitous C–H bonds in organic molecules is sustainable and atom-economical,<sup>2</sup> and in this respect, multiple unsymmetrical C–H bond functionalization

accomplished by a catalytic one-pot reaction is particularly attractive to furnish complex molecules from non-stereogenic simple starting materials. However, this can be daunting since chelation-assisted C–H bond activation is specific to DGs and catalysts,<sup>2f</sup> so the reaction conditions for the first C–H activation are often untenable for the next as the functional group (FG) introduced from the proceeding step might adversely affect subsequent C–H functionalization due to its electronic and/or steric effect. Therefore, such multiple C–H activation transformations can be tricky considering the different conditions needed for both activations.

The C(sp<sup>2</sup>)-H bond functionalization of *N*-phenoxyacetamides with various coupling partners has been successfully used in the synthesis of a broad spectrum of organic compounds,<sup>3</sup> due to the fact that the -ONHR moiety embedded in *N*-phenoxyamides can serve as not only a directing group but also an intramolecular oxidant. This unique feature eliminates the need for stoichiometric additional oxidants, allowing simplified reactivity and enhanced efficiency/selectivity. On the other hand, metal-carbenes generated from diazo compounds through facile extrusion of N<sub>2</sub> have been utilized as versatile coupling partners in C–H bond functionalization reactions of *N*-phenoxyamides.<sup>4</sup> In this regard, Wang and co-workers have developed a Rh(III)-catalyzed functionalization of

<sup>a</sup>Key Laboratory for Research and Evaluation of Innovative Drug, Key Laboratory of Green Chemical Media and Reactions, Ministry of Education, School of Environment, School of Chemistry and Chemical Engineering, Henan Normal University, Xinxiang, Henan 453007, China. E-mail: xinyingzhang@htu.cn, xuesen.fan@htu.cn

<sup>b</sup>School of Chemistry and Molecular Bioscience and Molecular Horizons, University of Wollongong, Northfields Avenue, Wollongong, NSW 2522, Australia. E-mail: richmond\_lee@uow.edu.au

†Electronic supplementary information (ESI) available. CCDC 2164269 (3a) 2164272 (5b) and 2164274 (10). For ESI and crystallographic data in CIF or other electronic format see DOI: <https://doi.org/10.1039/d2qo00851c>

*N*-phenoxyacetamides with diazoesters to give *ortho*-alkenyl phenols (Scheme 1a).<sup>4a</sup> Yi *et al.* reported a Rh(III)-catalyzed C–H bond insertion of *N*-phenoxyacetamides with  $\alpha$ -diazomalones to give 2-(2-hydroxyphenyl)-2-alkoxymalones (Scheme 1b).<sup>4b</sup> Liu *et al.* reported a Rh(III)-catalyzed reaction of *N*-aryloxyacetamides with 6-diazo-2-cyclohexenones to provide *ortho*-biphenols (Scheme 1c).<sup>4c</sup> In addition, Zhou *et al.* recently reported a one-pot unsymmetrical cascade C–H alkylation and amidation of *N*-phenoxyacetamides with  $\alpha$ -diazomalones (Scheme 1d).<sup>4d</sup>

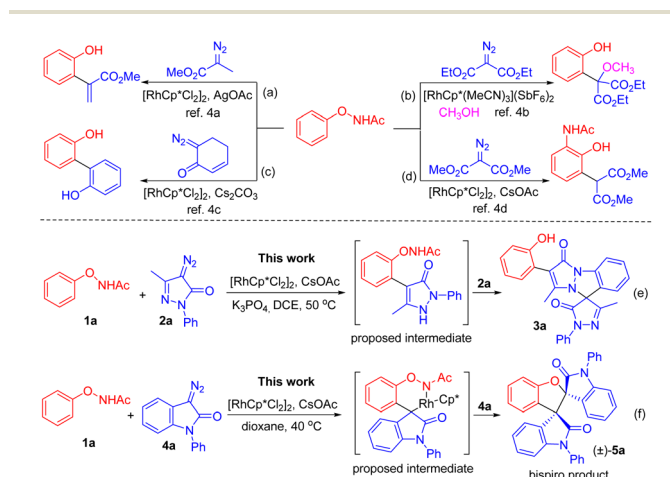
Inspired by these elegant pioneering studies and continuing our interest on the functionalization of inert chemical bonds,<sup>5,6</sup> in this work we endeavored to design and explore the reactions of *N*-phenoxyacetamides with diazopyrazolones<sup>7</sup> and diazooxindoles<sup>8</sup> with the aim of obtaining new chemical entities that have potential pharmaceutical and material applications. Serendipitously, we found two unprecedented distinct reaction modes of *N*-phenoxyacetamides under the catalysis of Rh(III). First, when 4-diazo-3-methyl-1-phenyl-1*H*-pyrazol-5(4*H*)-one (**2a**) was reacted with *N*-phenoxyacetamide (**1a**), a spiro-pyrazolonyl indazole derivative tethered with a phenol moiety (**3a**) was formed through cascade unsymmetrical C–H bond functionalization and carbene insertion (Scheme 1e). Interestingly, the first functionalization occurred on the phenyl ring of **1a** as expected while the second one took place unexpectedly on the phenyl ring of the *in situ* introduced 2-phenylpyrazolonyl moiety from **2a**. Second, when 3-diazo-1-phenylindolin-2-one (**4a**) was reacted with **1a**, a bispirooxindoyl dihydrobenzofuran derivative (**5a**) was obtained through one-pot C–H bond functionalization and double carbene insertion (Scheme 1f). The first insertion occurred on the phenyl ring of **1a** while the second one surprisingly took place on the *in situ* introduced oxindoyl moiety from **4a**, thus resulting in a novel [3 + 1 + 1] bispirocyclization of *N*-phenoxyacetamide with two diazooxindoles. It is worth noting that while sequential carbene insertions with diazo compounds as carbene precursors have been previously reported, they usually occur symmetrically on the two *ortho*-sites of the same substrates.<sup>4e,f</sup> To our

knowledge, the unsymmetrical reaction modes as shown in Scheme 1e and f have not been reported previously. In addition, the introduction of spiro moieties often effectively alters the physicochemical and biological properties of parent compounds due to the high rigidity and unique three-dimensional geometries of spiro structures. Among various spiro scaffolds, spiro-pyrazolones<sup>9</sup> and spirooxindoles<sup>10</sup> are ubiquitous in natural products, pharmaceuticals, agrochemicals, dyes and chelating agents (Fig. 1). Therefore, the development of novel methods for the preparation of spiro-pyrazolone and bispirooxindole derivatives from easily obtainable substrates through a simple operation is highly valuable.

## Results and discussion

Initially, a mixture of *N*-phenoxyacetamide (**1a**) and 4-diazo-3-methyl-1-phenyl-1*H*-pyrazol-5(4*H*)-one (**2a**) was treated with [RhCp\*Cl<sub>2</sub>]<sub>2</sub> and CsOAc in DCE at 50 °C for 24 h forming spiro-pyrazolonyl indazole **3a** in 25% yield (Table 1, entry 1). Encouraged by this result, a systematic optimization study was carried out. First, catalyst screening was conducted using [IrCp\*Cl<sub>2</sub>]<sub>2</sub>, CoCp\*(CO)I<sub>2</sub>, [RhCp\*(MeCN)<sub>3</sub>](SbF<sub>6</sub>)<sub>2</sub>, [Ru(*p*-cymene)Cl<sub>2</sub>]<sub>2</sub> and MnBr(CO)<sub>5</sub> (entries 2–6). The Rh complex [RhCp\*(MeCN)<sub>3</sub>](SbF<sub>6</sub>)<sub>2</sub> showed similar performance to [RhCp\*Cl<sub>2</sub>]<sub>2</sub> while others were not effective. When K<sub>3</sub>PO<sub>4</sub> was used as an additive with CsOAc, **3a** was formed in 65% yield (entry 7). Replacing K<sub>3</sub>PO<sub>4</sub> with KH<sub>2</sub>PO<sub>4</sub>, K<sub>2</sub>HPO<sub>4</sub> or KOAc decreased the yield (entries 8–10). Replacing CsOAc with CsF, Cs<sub>2</sub>CO<sub>3</sub>, CsOPiv, NaOAc, KOAc or AgOAc resulted in a lower reaction efficiency (entries 11–16). Subsequently, the effect of different solvents such as CHCl<sub>3</sub>, DCM, ethanol, MeCN, dioxane and PhCl was further investigated. They were inferior to DCE (entries 17–22). When it was performed at higher temperature, the yield of **3a** decreased obviously (entry 23). As a control experiment, **3a** was not formed in the absence of the Rh(III) catalyst (entry 24).

With the established optimal reaction conditions to give **3a**, the substrate scope of this reaction was expanded. First, diverse substituted *N*-phenoxyacetamides **1** were tested through their reactions with **2a** (Scheme 2), and it was found that the reactions of **1** bearing methyl, isopropyl, *tert*-butyl,



Scheme 1 Reactions of *N*-phenoxyacetamide with diazo compounds.

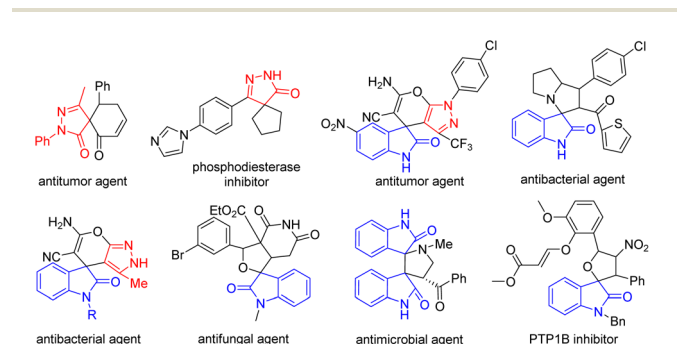
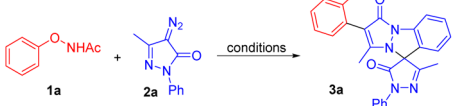


Fig. 1 Some important spiro-pyrazolone and spirooxindole derivatives.

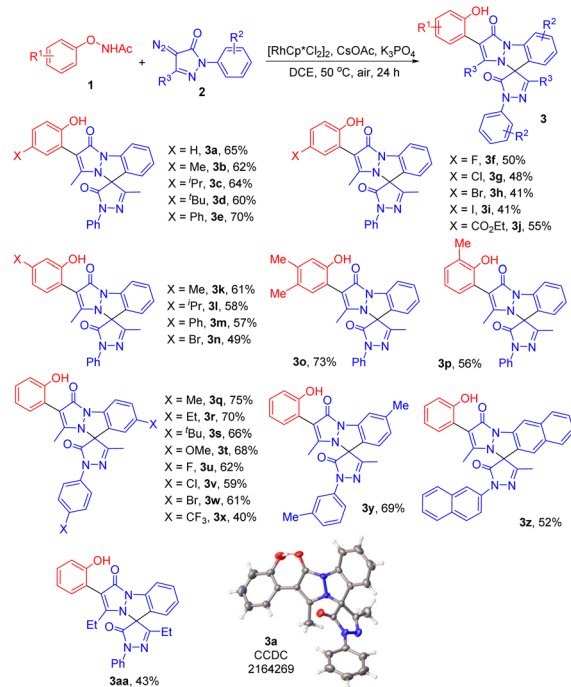
Table 1 Optimization study for the formation of **3a**<sup>a</sup>


Entry	Catalyst	Additive 1	Additive 2	Solvent	Yield <sup>b</sup> (%)
1	[RhCp*Cl <sub>2</sub> ] <sub>2</sub>	CsOAc		DCE	25
2	[IrCp*Cl <sub>2</sub> ] <sub>2</sub>	CsOAc		DCE	Trace
3	CoCp*(CO) <sub>2</sub>	CsOAc		DCE	ND
4	[RhCp*(MeCN) <sub>3</sub> ] (SbF <sub>6</sub> ) <sub>2</sub>	CsOAc		DCE	23
5	[Ru( <i>p</i> -cymene)Cl <sub>2</sub> ] <sub>2</sub>	CsOAc		DCE	ND
6	MnBr(CO) <sub>5</sub>	CsOAc		DCE	ND
7	[RhCp*Cl <sub>2</sub> ] <sub>2</sub>	CsOAc	K <sub>3</sub> PO <sub>4</sub>	DCE	65
8	[RhCp*Cl <sub>2</sub> ] <sub>2</sub>	CsOAc	KH <sub>2</sub> PO <sub>4</sub>	DCE	48
9	[RhCp*Cl <sub>2</sub> ] <sub>2</sub>	CsOAc	K <sub>2</sub> HPO <sub>4</sub>	DCE	39
10	[RhCp*Cl <sub>2</sub> ] <sub>2</sub>	CsOAc	KOAc	DCE	39
11	[RhCp*Cl <sub>2</sub> ] <sub>2</sub>	CsF	K <sub>3</sub> PO <sub>4</sub>	DCE	25
12	[RhCp*Cl <sub>2</sub> ] <sub>2</sub>	Cs <sub>2</sub> CO <sub>3</sub>	K <sub>3</sub> PO <sub>4</sub>	DCE	Trace
13	[RhCp*Cl <sub>2</sub> ] <sub>2</sub>	CsOPiv	K <sub>3</sub> PO <sub>4</sub>	DCE	ND
14	[RhCp*Cl <sub>2</sub> ] <sub>2</sub>	NaOAc	K <sub>3</sub> PO <sub>4</sub>	DCE	33
15	[RhCp*Cl <sub>2</sub> ] <sub>2</sub>	KOAc	K <sub>3</sub> PO <sub>4</sub>	DCE	25
16	[RhCp*Cl <sub>2</sub> ] <sub>2</sub>	AgOAc	K <sub>3</sub> PO <sub>4</sub>	DCE	21
17	[RhCp*Cl <sub>2</sub> ] <sub>2</sub>	CsOAc	K <sub>3</sub> PO <sub>4</sub>	CHCl <sub>3</sub>	30
18	[RhCp*Cl <sub>2</sub> ] <sub>2</sub>	CsOAc	K <sub>3</sub> PO <sub>4</sub>	DCM	28
19	[RhCp*Cl <sub>2</sub> ] <sub>2</sub>	CsOAc	K <sub>3</sub> PO <sub>4</sub>	EtOH	Trace
20	[RhCp*Cl <sub>2</sub> ] <sub>2</sub>	CsOAc	K <sub>3</sub> PO <sub>4</sub>	MeCN	Trace
21	[RhCp*Cl <sub>2</sub> ] <sub>2</sub>	CsOAc	K <sub>3</sub> PO <sub>4</sub>	Dioxane	Trace
22	[RhCp*Cl <sub>2</sub> ] <sub>2</sub>	CsOAc	K <sub>3</sub> PO <sub>4</sub>	PhCl	Trace
23 <sup>c</sup>	[RhCp*Cl <sub>2</sub> ] <sub>2</sub>	CsOAc	K <sub>3</sub> PO <sub>4</sub>	DCE	55
24	[RhCp*Cl <sub>2</sub> ] <sub>2</sub>	CsOAc	K <sub>3</sub> PO <sub>4</sub>	DCE	ND

<sup>a</sup> Reaction conditions: **1a** (0.2 mmol), **2a** (0.44 mmol), catalyst (2.5 mol%), additive 1 (0.2 mmol), additive 2 (0.2 mmol), solvent (2 mL), 50 °C, air, 24 h. <sup>b</sup> Isolated yields. <sup>c</sup> 60 °C.

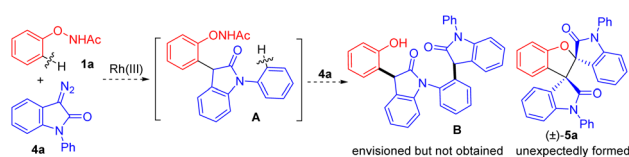
phenyl, fluoro, chloro, bromo, iodo or ester groups on the *para*-position of its phenyl moiety proceeded smoothly to afford products **3b–3j**. Notably, chemically active disubstituted *N*-phenoxyacetamide reacted with **2a** to furnish **3o** in good yield. When *ortho*-substituted *N*-phenoxyacetamide was tried, the desired reaction took place smoothly to give **3p**. Furthermore, the suitability of an array of diverse substituted diazopyrazolones **2** was studied using **1a** as a model substrate. It was observed that diazopyrazolones **2** bearing methyl, ethyl, *tert*-butyl, methoxy, fluoro, chloro, bromo or trifluoromethyl units on different sites of their *N*-phenyl moiety were viable coupling partners to afford **3q–3y** in moderate to good yields. Notably, no obvious electronic or steric effect was observed in these cases. In addition to the phenyl unit, the diazopyrazolone bearing the *N*-naphthyl moiety took part in this reaction to give **3z**. Changing the R<sup>3</sup> unit on the pyrazolonyl ring from methyl to ethyl led to **3aa**. Notably, the structure of **3a** was unambiguously confirmed by single-crystal X-ray diffraction analysis.

Thus far, we have established an effective and easy synthesis of spiro-pyrazolonyl indazoles **3** from the cascade reaction of *N*-phenoxyacetamides **1** with diazopyrazolones **2**. Based on the structure of **3**, it was deduced that cascade unsymmetri-



**Scheme 2** Substrate scope for the synthesis of **3**. Reaction conditions: **1** (0.2 mmol), **2** (0.44 mmol), [RhCp\*Cl<sub>2</sub>]<sub>2</sub> (2.5 mol%), CsOAc (0.2 mmol), K<sub>3</sub>PO<sub>4</sub> (0.2 mmol), DCE (2 mL), 50 °C, air, 24 h. Isolated yield.

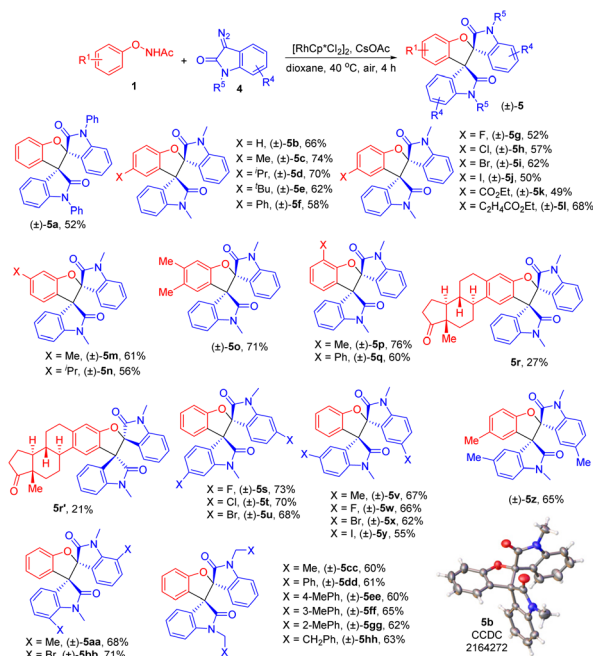
cal C(sp<sup>2</sup>)-H bond functionalization and carbene insertion reactions must have occurred on different phenyl units during their formation, first on the phenyl ring of **1** and second on the phenyl ring of the *N*-phenylpyrazolonyl moiety *in situ* introduced from **2**, using the NH unit as a DG. Inspired by this intriguing result, we were then interested in testing the suitability of other kinds of cyclic diazo compounds as possible coupling partners with the aim to broaden the horizon of this unsymmetrical C-H functionalization strategy. Thus, we chose to react **1a** with 3-diazo-1-phenylindolin-2-one (**4a**). It was envisioned that **1a** might first react with **4a** to give **A** via *ortho*-C-H activation and carbene insertion on the phenyl ring of **1a** (Scheme 3). Under the reaction conditions, **A** might continue to undergo the second C-H bond activation and carbene insertion with **4a** on the *ortho*-position of the *N*-phenyl ring of the *in situ* introduced indolinone moiety using the carbonyl unit of indolinone as a weakly coordinating DG to give the bisindolinone derivative **B**.



**Scheme 3** Envisioned reaction of *N*-phenoxyacetamide with 3-diazo-1-phenylindolin-2-one.

To test the feasibility of the reaction proposed in Scheme 3, a mixture of **1a** and **4a** was subjected to the standard conditions used in Scheme 2. Under this circumstance, however, the formation of the envisioned product **B** was not detected. Meanwhile, a bispirooxindoyl dihydrobenzofuran derivative **5a** was isolated (Scheme 3). Even though in low yield, the serendipitous formation of **5a** aroused our strong interest as an alternative cascade process of C–H bond activation and unsymmetrical carbene insertions should have occurred, first on the phenyl ring of **1a** and second on the C3 position of the *in situ* introduced oxindoyl moiety rather than its *N*-phenyl unit. As a sequential construction of vicinal spiro centers is considerably challenging due to their high steric hindrance, the formation of **5a** is mechanistically and synthetically promising. In addition, the dihydrobenzofuran moiety is common in natural products and synthetic compounds possessing significant antidepressant, antifungal, antitubercular, antitussive, opioid analgesic, opioid antagonizing, antiarrhythmic and antiproliferative activities.<sup>11</sup> While a number of synthetic methods have been reported for the synthesis of benzofuran derivatives,<sup>11,12</sup> there is still no precedent for the diastereoselective synthesis of bispirooxindoyl benzofurans starting from acyclic substrates. Therefore, the rapid assembly of structurally complex molecules like **5a** will be attractive.

To translate this serendipitous finding into an effective and reliable synthetic protocol, systematic screening of the parameters possibly affecting the reaction efficiency was carried out using the more economical 3-diazo-1-methylindolin-2-one (**4b**) as a model coupling partner to react with **1a**. It was thus found that by treating **1a** with **4b** in the presence of [RhCp\*Cl<sub>2</sub>]<sub>2</sub> (7 mol%) and CsOAc (10 mol%) in dioxane (2 mL) at 40 °C in air for 4 h, the desired product **5b** was obtained in 66% yield and its structure was unambiguously confirmed by single-crystal X-ray diffraction analysis (Scheme 4). In follow-up studies, the scope of *N*-phenoxyacetamides **1** for the formation of **5** was thoroughly explored. The results included in Scheme 4 showed that **1**, attached with either an electron-donating group including methyl, isopropyl, *tert*-butyl, phenyl or an electron-withdrawing group such as fluoro, chloro, bromo, iodo, or ester on the *para* position of the phenyl ring, reacted with **4b** efficiently to afford **5c–5k** in moderate to good yields. The compatibility of bromo, iodo and ester groups allows for further product scope. Interestingly, **1** bearing a chain ester unit gave **5l** in reasonably good yield. Notably, the reactions of *meta*-methyl or *meta*-isopropyl substituted *N*-phenoxyacetamides occurred regioselectively on the less hindered site to give **5m**, **5n** and **5o**. When *ortho*-substituted *N*-phenoxyacetamides were tried, the desired products **5p** and **5q** were formed smoothly. The *N*-phenoxyacetamide substrate derived from estrone was found to be also compatible with this spiroannulation reaction to give diastereoisomeric pairs **5r** and **5r'**, indicating that this reaction can be applied for the late-stage assembly of bioactive complexes. Next, the generality of diazooxindoles **4** as coupling partners for this reaction was studied. The diazooxindole **4** bearing a methyl, fluoro, chloro, bromo or iodo unit on different sites of the oxindole scaffold

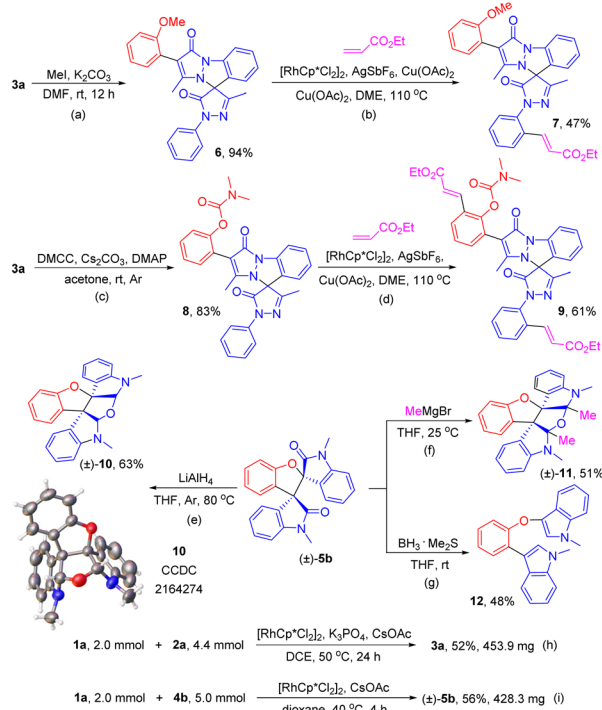


**Scheme 4** Substrate scope for the synthesis of **5**. Reaction conditions: **1** (0.2 mmol), **4** (0.5 mmol), [RhCp\*Cl<sub>2</sub>]<sub>2</sub> (7 mol%), CsOAc (10 mol%), dioxane (2 mL), 40 °C, air, 4 h. Isolated yield.

competently reacted with **1a** to form the desired products **5s–5bb** in moderate to good yields with no deleterious electronic or steric effect. Diazooxindoles **4** bearing various *N*-alkyl substituents other than the methyl unit were also used. It was found that *N*-ethyl, benzyl, 4-methylbenzyl, 3-methylbenzyl, 2-methylbenzyl and 2-phenylethyl substituted diazo oxindoles reacted with **1a** smoothly to give **5cc–5hh** in comparable efficiencies.

To demonstrate the synthetic utility of the products, further transformations of **3a** and **5b** were conducted and the results are shown in Scheme 5. First, **3a** was treated with methyl iodide in the presence of K<sub>2</sub>CO<sub>3</sub> in DMF to give the anisole derivative **6**. Next, Rh(III)-catalyzed C–H olefination of **6** with ethyl acrylate furnished product **7**. On the other hand, **3a** was treated with dimethyl carbamoyl chloride (DMCC) in the presence of Cs<sub>2</sub>CO<sub>3</sub> and DMAP to afford the carbamate derivative **8**. Furthermore, Rh(III)-catalyzed C–H olefination of **8** with ethyl acrylate gave a doubly functionalized product **9**.<sup>13</sup> As another aspect, when product **5b** was treated with LiAlH<sub>4</sub>, a structurally unique heptacyclic product **10** was formed with good efficiency. Notably, the structure of **10** was unambiguously confirmed by X-ray diffraction analysis. In addition, reacting **5b** with MeMgBr gave another heptacyclic product **11** bearing four fully substituted carbon centers. In addition, through the reaction of **5b** with BH<sub>3</sub>·Me<sub>2</sub>S, product **12** was generated through carbonyl reduction and C–C bond cleavage. Finally, larger-scale syntheses of **3a** and **5b** were also carried out, in which 2 mmol of **1a** was treated with 4.4 mmol of **2a** under standard conditions to afford **3a** in 52% yield, and

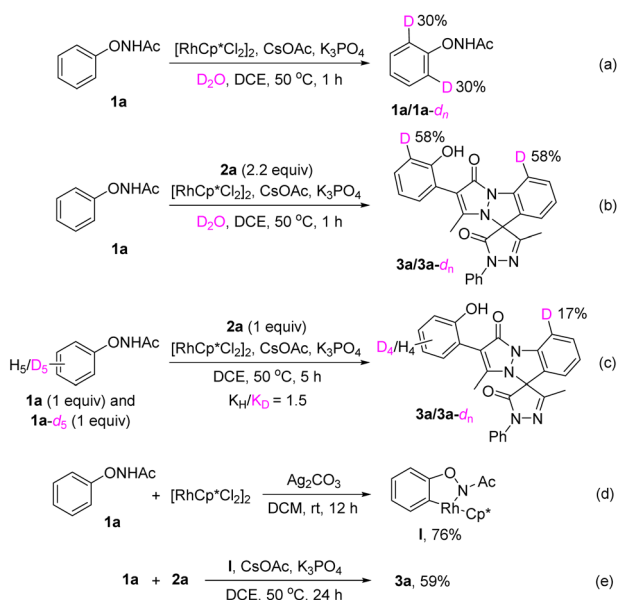




**Scheme 5** Structural elaborations of **3a** and **5b** and enlarged scale preparations.

2 mmol of **1a** was treated with 5 mmol of **4b** to furnish **5b** in 56% yield (also shown in Scheme 5).

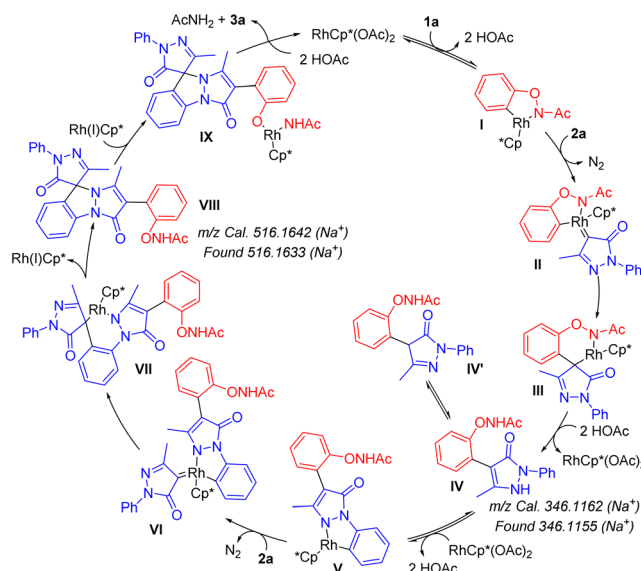
Experimental mechanistic studies were performed to understand how **3a** was generated. Compound **1a** was subjected to standard conditions in the presence of 10 equiv. of  $\text{D}_2\text{O}$  for 1 h. As a result, 30% H/D exchange at the *ortho*-positions of



**Scheme 6** Mechanistic studies.

the phenyl ring of **1a** was observed, suggesting that C–H activation has occurred under the catalysis of the Rh(III) catalyst (Scheme 6a). When the reaction of **1a** with **2a** was carried out in the presence of 10 equiv. of  $\text{D}_2\text{O}$  for 1 h, deuterium incorporations were also observed in **3a**, revealing that the C–H activation process might be reversible (Scheme 6b). Kinetic isotopic effect (KIE) studies were performed by treating an equimolar mixture of **1a/1a- $d_5$**  with **2a** under standard conditions for 5 h (Scheme 6c). A  $k_{\text{H}}/k_{\text{D}}$  value of 1.5 indicated that the first C–H bond activation might not be involved in the rate-limiting step in the formation of **3a**. Furthermore, when **1a** was reacted with  $[\text{RhCp}^*\text{Cl}_2]_2$  in the presence of  $\text{Ag}_2\text{CO}_3$  in  $\text{CH}_2\text{Cl}_2$  at ambient temperature for 12 h, a rhodacycle species **I** was obtained in 76% yield (Scheme 6d).<sup>14</sup> Using **I** as a catalyst, the reaction of **1a** with **2a** afforded **3a** in 59% yield, indicating that **I** might have been involved in the formation of **3a** (Scheme 6e).

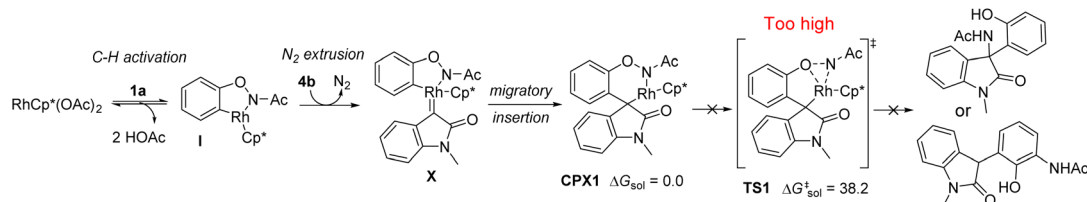
With support from the experimental work and literature reports,<sup>4</sup> a plausible mechanism for the formation of **3a** from the reaction of **1a** with **2a** is shown in Scheme 7. First, the ligand exchange of the  $[\text{RhCp}^*\text{Cl}_2]_2$  complex with  $\text{CsOAc}$  forms  $\text{RhCp}^*(\text{OAc})_2$ , which activates the *ortho*-C–H bond of **1a** to furnish a rhodacycle intermediate **I**. Intermediate **I** further reacts with **2a** to form Rh carbene **II** through dediazonization. Migratory insertion of the Rh=C bond into the Rh–aryl bond expands the ring to a 6-membered intermediate **III**. Protonation of **III** with HOAc affords intermediate **IV** and regenerates the Rh(III) catalyst. The next C–H bond activation takes place on the *ortho*-position of the *N*-phenyl moiety of intermediate **IV** using the –NH moiety as a directing group, which proceeds to furnish another rhodacycle intermediate **V**. The extrusion of  $\text{N}_2$  from **2a** by reacting with **V** forms complex **VI**. Migratory insertion of the Rh=C bond into the Rh–aryl bond affords intermediate **VII**, and a reductive elimination



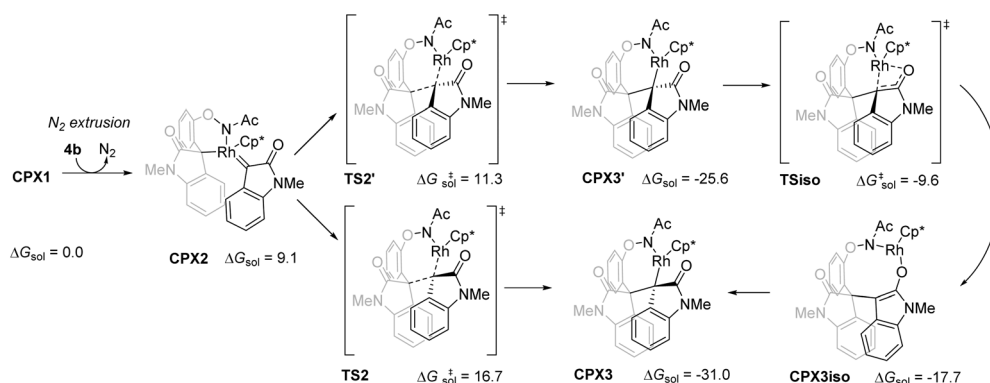
**Scheme 7** Proposed mechanism accounting for the formation of **3a**.

occurs with **VII** to give **VIII** and a Rh(I) species. Oxidative insertion of Rh(I) into the N–O bond of **VIII** furnishes intermediate **IX**. Protonation of **IX** affords product **3a**, AcNH<sub>2</sub> and the regenerated Rh(III) catalyst. The formation of intermediates **IV** and

**VIII** as proposed in Scheme 7 was supported by the HRMS analysis of the resulting mixture of the reaction between **1a** and **2a** under the standard conditions for 10 h (see the ESI† for details).



**Scheme 8** A DFT model for single **4b** addition products. Solution free energies in kcal mol<sup>-1</sup> relative to CPX1.



**Scheme 9** A DFT model for **4b** addition. Solution free energies in kcal mol<sup>-1</sup> relative to CPX1.

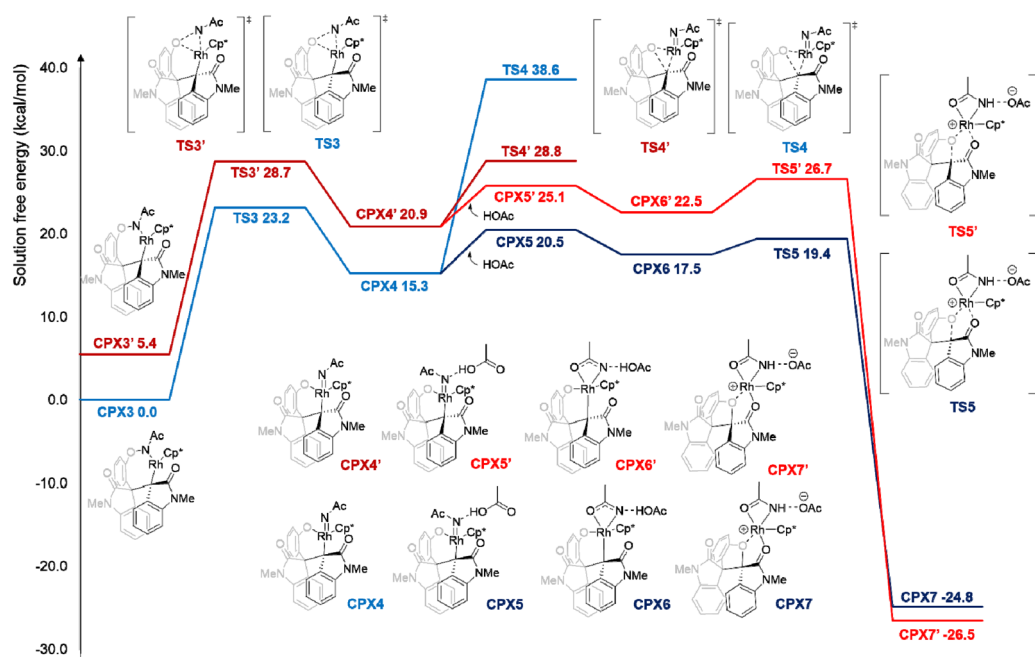


**Fig. 2** DFT calculations predicting the mechanism and diastereo-selective transformation of CPX3/CPX3'. Solution free energies in kcal mol<sup>-1</sup> relative to CPX3.

To unveil the reaction mechanism and the origin of chemoselectivity and diastereoselectivity for the formation of **5b** from the reaction of **1a** with **4b**, calculations were carried out (see ESI† mechanism prediction and density functional theory (DFT) for full computational details). First, the *in situ* generated intermediate **I** reacts with **4b** to form Rh carbene **X**, and subsequent migratory insertion affords **CPX1** (Scheme 8). Oxidative addition of Rh(III) into the O–N bond through **TS1** is high in the solution free energy barrier,  $\Delta G_{\text{sol}}^{\ddagger} = 38.2 \text{ kcal mol}^{-1}$ , thus eliminating the possibility of forming single carbene addition products.<sup>4</sup>

Complex **CPX1** can further react with **4b** to form the carbene complex **CPX2**, which is endergonic (Scheme 9),  $\Delta G_{\text{sol}} = 9.1 \text{ kcal mol}^{-1}$ , relative to **CPX1**. Migratory insertion of **CPX2** may result in diastereomers **CPX3** and **CPX3'** through the calculated transition states **TS2** and **TS2'**, respectively. Although the solution free energy of **TS2'** is lower than that of **TS2** by  $5.4 \text{ kcal mol}^{-1}$ , it is possible that **CPX3'** can still isomerize through **TSiso** and **CPX3iso** to convert to the more energetically stable diastereomer **CPX3**,  $\Delta G_{\text{sol}} = -31.0 \text{ kcal mol}^{-1}$  relative to **CPX1** (Scheme 9).

From Fig. 2, DFT calculations for the oxidative addition of Rh(III) into the N–O bond of **CPX3** or the diastereomer **CPX3'** reveal a free energy barrier of  $23.2 \text{ kcal mol}^{-1}$  through **TS3** and the much higher  $28.7 \text{ kcal mol}^{-1}$  through **TS3'** to form Rh(V) complexes **CPX4** and **CPX4'** (energies relative to **CPX3**). The ring-closure and concomitant reductive elimination through **TS4** and **TS4'** were calculated to be highly energetic at  $38.6$  and  $28.8 \text{ kcal mol}^{-1}$ , respectively. To aid in the ring-closure, it is postulated that addition of HOAc can make Rh(V) more electron-deficient and result in easier reductive elimination. On this note, complexation of **CPX4** and **CPX4'** with HOAc forms H-bonded **CPX5** and **CPX5'** and subsequently  $\eta^2$  N–Ac ligated **CPX6** and **CPX6'**. The reductive elimination from **CPX6** or **CPX6'** leads to **TS5** or **TS5'**,  $\Delta G_{\text{sol}}^{\ddagger} = 19.4$  or  $26.7 \text{ kcal mol}^{-1}$  relative to **CPX3**, respectively. The reductive elimination through **TS5** assisted by HOAc is indeed lower in energy as compared to **TS4** or **TS4'**, which leads to **CPX7**. Protodemetalation of **CPX7** affords the major diastereomer product **5b** as corroborated by the experimental X-ray single-crystal structure.

## Conclusions

We have developed coupling partner-controlled C–H bond functionalization and carbene insertion reactions of *N*-phenoxyacetamide with diazopyrazolones and diazooxindoles. From these reactions, structurally unique and biologically valuable spiro-pyrazolonyl indazole and bispirooxindoyl dihydrobenzofuran derivatives were effectively prepared in an atom-economical manner. Notably, these one-pot cascade C–H functionalization and sequential carbene insertion reactions took place on different cyclic systems, thus establishing successful examples of unsymmetrical C–H bond functionalization. Mechanistic experiments and DFT calculations helped to unveil the reaction mechanism and to clarify the excellent

chemoselectivity and diastereoselectivity demonstrated in these reactions. Further transformations of the products provided facile synthetic routes towards sophisticated architectures including heptacyclic scaffolds bearing four fully substituted carbon centers. These synthetic transformations will be valuable for drug discovery chemistry and related areas.

## Data availability

All experimental data and detailed experimental procedures are available in the ESI.†

## Author contributions

X. S. and X. F. conceived and designed the research. X. S., K. W. and L. X. performed the experiments. H. Y. and R. L. performed the theoretical calculations. X. S., X. Z. and X. F. analyzed the experimental data. X. S., X. Z., R. L. and X. F. wrote the manuscript.

## Conflicts of interest

The authors declare no competing financial interest.

## Acknowledgements

We are grateful to the National Natural Science Foundation of China (U2004189), the Project of Central Plains Science and Technology Innovation Leading Talents (224200510009), the Program for Innovative Research Team in Science and Technology in Universities of Henan Province (20IRTSTHN005) and the Henan Key Laboratory of Organic Functional Molecules and Drug Innovation for financial support. R. L. gratefully acknowledges generous allocations of supercomputing time on the National Facility of the National Computational Infrastructure (Australia) and financial support from the Australian Research Council (DE210100053, R. L.), UOW RITA Grant 2021 (R. L. and H. Y.) and a UOW Vice Chancellor's Research Fellowship (R. L.).

## Notes and references

- (a) C. M. R. Volla, I. Atodiresei and M. Rueping, *Chem. Rev.*, 2014, **114**, 2390–2431; (b) S. Kar, H. Sanderson, K. Roy, E. Benfenati and J. Leszczynski, *Chem. Rev.*, 2022, **122**, 3637–3710; (c) Y. Wang, H. Lu and P.-F. Xu, *Acc. Chem. Res.*, 2015, **48**, 1832–1844.
- (a) C. Sambiagio, D. Schönbauer, R. Blicke, T. Dao-Huy, G. Pototschnig, P. Schaaf, T. Wiesinger, M. F. Zia, J. Wencel-Delord, T. Besset, B. U. Maes and W. M. Schnürch, *Chem. Soc. Rev.*, 2018, **47**, 6603–6743; (b) P. Gandeepan, T. Müller, D. Zell, G. Cera, S. Warratz

- and L. Ackermann, *Chem. Rev.*, 2019, **119**, 2192–2452; (c) S. Rej and N. Chatani, *Angew. Chem., Int. Ed.*, 2019, **58**, 8304–8329; (d) Y. Wu, C. Pi, Y. Wu and X. Cui, *Chem. Soc. Rev.*, 2021, **50**, 3263–3314; (e) S. Rej, A. Das and N. Chatani, *Coord. Chem. Rev.*, 2021, **431**, 213683–213719; (f) B. Liu, L. Yang, P. Li, F. Wang and X. Li, *Org. Chem. Front.*, 2021, **8**, 1085–1101; (g) K. Ghosh, R. K. Rit, E. Ramesh and A. K. Sahoo, *Angew. Chem., Int. Ed.*, 2016, **55**, 7821–7825.
- 3 (a) P. Duan, Y. Yang, R. Ben, Y. Yan, L. Dai, M. Hong, Y.-D. Wu, D. Wang, X. Zhang and J. Zhao, *Chem. Sci.*, 2014, **5**, 1574–1578; (b) Z. Zhou, G. Liu, Y. Chen and X. Lu, *Org. Lett.*, 2015, **17**, 5874–5877; (c) X. Wang, A. Lerchen, C. G. Daniliuc and F. Glorius, *Angew. Chem., Int. Ed.*, 2018, **57**, 1712–1716; (d) W. Yi, W. Chen, F.-X. Liu, Y. Zhong, D. Wu, Z. Zhou and H. Gao, *ACS Catal.*, 2018, **8**, 9508–9519; (e) J.-L. Pan, P. Xie, C. Chen, Y. Hao, C. Liu, H.-Y. Bai, J. Ding, L.-R. Wang, Y. Xia and S.-Y. Zhang, *Org. Lett.*, 2018, **20**, 7131–7136; (f) H. Gao, M. Sun, H. Zhang, M. Bian, M. Wu, G. Zhu, Z. Zhou and W. Yi, *Org. Lett.*, 2019, **21**, 5229–5233; (g) J.-L. Pan, C. Liu, C. Chen, T.-Q. Liu, M. Wang, Z. Sun and S.-Y. Zhang, *Org. Lett.*, 2019, **21**, 2823–2827; (h) G. Zheng, Z. Zhou, G. Zhu, S. Zhai, H. Xu, X. Duan, W. Yi and X. Li, *Angew. Chem., Int. Ed.*, 2020, **59**, 2890–2896; (i) X. Zhong, S. Lin, H. Gao, F.-X. Liu, Z. Zhou and W. Yi, *Org. Lett.*, 2021, **23**, 2285–2291; (j) K. Chen, W. Chen, F. Chen, H. Zhang, H. Xu, Z. Zhou and W. Yi, *Org. Chem. Front.*, 2021, **8**, 4452–4458; (k) L. Wu, H. Xu, H. Gao, L. Li, W. Chen, Z. Zhou and W. Yi, *ACS Catal.*, 2021, **11**, 2279–2287; (l) L. Wu, L. Li, H. Zhang, H. Gao, Z. Zhou and W. Yi, *Org. Lett.*, 2021, **23**, 3844–3849; (m) K. Ozols, S. Onodera, Ł. Woźniak and N. Cramer, *Angew. Chem., Int. Ed.*, 2021, **60**, 655–659.
- 4 (a) F. Hu, Y. Xia, F. Ye, Z. Liu, C. Ma, Y. Zhang and J. Wang, *Angew. Chem., Int. Ed.*, 2014, **53**, 1364–1367; (b) J. Zhou, J. Shi, X. Liu, J. Jia, H. Song, H. E. Xu and W. Yi, *Chem. Commun.*, 2015, **51**, 5868–5871; (c) Z. Hu and G. Liu, *Adv. Synth. Catal.*, 2017, **359**, 1643–1648; (d) Y. Wu, Z. Chen, Y. Yang, W. Zhu and B. Zhou, *J. Am. Chem. Soc.*, 2018, **140**, 42–45; (e) S. Nunewar, S. Kumar, S. Talakola, S. Nanduri and V. Kanchupalli, *Chem. – Asian J.*, 2021, **16**, 443–459; (f) N. Jha, N. Khot and M. Kapur, *Chem. Rec.*, 2021, **21**, 4088–4122.
- 5 (a) B. Li, B. Zhang, X. Zhang and X. Fan, *Chem. Commun.*, 2017, **53**, 1297–1300; (b) G. Chen, X. Zhang, R. Jia, B. Li and X. Fan, *Adv. Synth. Catal.*, 2018, **360**, 3781–3787; (c) X. Chen, M. Wang, X. Zhang and X. Fan, *Org. Lett.*, 2019, **21**, 2541–2545; (d) C. Gao, B. Li, X. Geng, Q. Zhou, X. Zhang and X. Fan, *Green Chem.*, 2019, **21**, 5113–5117; (e) X. Song, X. Cai, X. Zhang and X. Fan, *Org. Chem. Front.*, 2021, **8**, 6265–6272.
- 6 (a) X. Song, B. N. D. Doan, X. Zhang, R. Lee and X. Fan, *Org. Lett.*, 2020, **22**, 46–51; (b) Q. Zhou, X. Song, X. Zhang and X. Fan, *Org. Chem. Front.*, 2021, **8**, 4131–4137; (c) M. Wang, L. Zhang, X. Chen, X. Zhang and X. Fan, *Org. Chem. Front.*, 2021, **8**, 3238–3243; (d) Q. Zhou, X. Song, X. Zhang and X. Fan, *Org. Lett.*, 2022, **24**, 1280–1285.
- 7 (a) R. P. Pandita and Y. R. Lee, *Adv. Synth. Catal.*, 2015, **357**, 2657–2664; (b) F. Fang, S. Hu, C. Li, Q. Wang, R. Wang, X. Han, Y. Zhou and H. Liu, *Angew. Chem., Int. Ed.*, 2021, **60**, 21327–21333.
- 8 (a) T. K. Hyster, K. E. Ruhl and T. Rovis, *J. Am. Chem. Soc.*, 2013, **135**, 5364–5367; (b) B. Ma, P. Wu, X. Wang, Z. Wang, H.-X. Lin and H.-X. Dai, *Angew. Chem., Int. Ed.*, 2019, **58**, 13335–13339.
- 9 (a) J.-Y. Liang, S.-J. Shen, X.-Q. Chai and T. Lv, *J. Org. Chem.*, 2018, **83**, 12744–12752; (b) Y. Lin, B.-L. Zhao and D.-M. Du, *J. Org. Chem.*, 2019, **84**, 10209–10220; (c) M. J. Sarma, S. Jindani, B. Ganguly, S. Pabbaraja and G. Mehta, *J. Org. Chem.*, 2022, **87**, 884–891.
- 10 (a) G. S. Singh and Z. Y. Desta, *Chem. Rev.*, 2012, **112**, 6104–6155; (b) Z.-Y. Cao, F. Zhou and J. Zhou, *Acc. Chem. Res.*, 2018, **51**, 1443–1454; (c) A. Ding, M. Meazza, H. Guo, J. W. Yang and R. Rios, *Chem. Soc. Rev.*, 2018, **47**, 5946–5996; (d) J. Bariwal, L. G. Voskressensky and E. V. Van der Eycken, *Chem. Soc. Rev.*, 2018, **47**, 3831–3848; (e) X. Zhang, Y. Gao, Y. Liu and Z. Miao, *J. Org. Chem.*, 2021, **86**, 8630–8640; (f) A. J. Boddy and J. A. Bull, *Org. Chem. Front.*, 2021, **8**, 1026–1084.
- 11 (a) R. J. Nevagi, S. N. Dighe and S. N. Dighe, *Eur. J. Med. Chem.*, 2015, **97**, 561–581; (b) T. Smith, E. Vitaku and J. T. Njardarson, *Org. Lett.*, 2017, **19**, 3508–3511 and references cited therein; (c) N. Cardullo, L. Pulvirenti, C. Spatafora, N. Musso, V. Barresi, D. F. Condorelli and C. Tringali, *J. Nat. Prod.*, 2016, **79**, 2122–2134.
- 12 (a) H. Wang, G. Li, K. M. Engle, J.-Q. Yu and H. M. L. Davies, *J. Am. Chem. Soc.*, 2013, **135**, 6774–6777; (b) L. Qin, D.-D. Vo, A. Nakhai, C. D. Andersson and M. Elofsson, *ACS Comb. Sci.*, 2017, **19**, 370–376; (c) S. Xie, Y. Li, P. Liu and P. Sun, *Org. Lett.*, 2020, **22**, 8774–8779; (d) Z. Lu, Q. Zhang, M. Ke, S. Hu, X. Xiao and F. Chen, *J. Org. Chem.*, 2021, **86**, 7625–7635; (e) L. Liu, F. Cheng, C. Meng, A.-A. Zhang, M. Zhang, K. Xu, N. Ishida and M. Murakami, *ACS Catal.*, 2021, **11**, 8942–8947; (f) Z.-R. Jing, D.-D. Liang, J.-M. Tian, F.-M. Zhang and Y.-Q. Tu, *Org. Lett.*, 2021, **23**, 1258–1262.
- 13 (a) T.-J. Gong, B. Xiao, Z.-J. Liu, J. Wan, J. Xu, D.-F. Luo, Y. Fu and L. Liu, *Org. Lett.*, 2011, **13**, 3235–3237; (b) C. Pan, S.-Y. Yin, S.-B. Wang, Q. Gu and S.-L. You, *Angew. Chem., Int. Ed.*, 2021, **60**, 15510–15516.
- 14 Q. Wu, Y. Chen, D. Yan, M. Zhang, Y. Lu, W.-Y. Sun and J. Zhao, *Chem. Sci.*, 2017, **8**, 169–173.